Discoid solitons and solitary wave trains in an expanding collisionless local universe

Tzihong Chiueh and Tak-Pong Woo

Institute of Astronomy and Department of Physics, National Central University, Chung-Li, Taiwan

(Received 14 June 1996)

Nonlinear gravitational sound waves within an expanding collisionless background matter are investigated. Under the assumptions of power-law time dependence and an equation of state for collisionless particles, two classes of nonlinear waves are identified: solitons and solitary wave trains. The soliton solutions may describe physically how the high-density sheets evolve immediately after the formation of caustics in the disk-collapse scenario of large-scale structure formation. The solutions can describe either that a discoid continuously loses matter that is expelled by the high pressure of the disk, reaching supersonic speeds and presumably blended into the background Hubble flow, or that the disk collects matter from the low-density background and becomes ever-increasingly massive. We also find that the multiple-mass-shell solutions, generally believed to be caused by the crossing of mass shells after the gravitational collapse, exist in the form of solitons. [S1063-651X(97)02701-3]

PACS number(s): 03.40.Kf, 04.40.−b, 95.35.+d, 98.65.Dx

I. INTRODUCTION

Collisionless dark matter increasingly has been believed to contribute to the majority of gravitational masses in the Universe. (For a review see [1].) In the hope of extracting some useful information about the dark matter, we investigated the wave characteristics in these collisionless particles in a previous work [2]. It is well known that the Newtonian theory of gravity is sufficient to describe the general gravitational dynamics as long as the temperature of the matter is nonrelativistic and the length scale well below the size of the horizon [3]. In our previous work, the focus was placed on waves in a *static* background within the framework of the Newtonian theory. It was concluded that all gravitational sound wave solutions in a static background were not physical. (See the Appendix for a brief description of that work [2].)

The present work is motivated by the notion that it is only when the background is not static can the matter, in the presence of self-gravity, be distributed uniformly. Such a nonstatic background may provide suitable support for waves to exist. Moreover, observational evidence has accumulated recently and indicates that the matter density of the local universe, including the dark matter, is less, by a sizable margin, than the critical density $\rho_c \equiv 1/6\pi G t^2$, above which the expansion of the universe will be halted by gravity [4,5]. We are also motivated by these observations and attempt to examine how nonlinear structures, including waves, may evolve in an underdense universe.

More importantly, we note that the disk collapse is probably inevitable in the processes of structure formation for scales of superclusters [6–11]. It is thus relevant to understand how nonlinear evolution may proceed analytically, as opposed to numerically as pursued by most investigators. (See, for example, [12] for a brief summary of a certain class of simulations.) Mass-shell crossings have been proposed as the basic mechanisms yielding collisionless gravitational turbulence and producing small-scale structures [13,14]. In particular, multiple-mass-shell configurations also have been observed in numerical studies and considered to be one of

the key features in collisionless gravitational turbulence [15]. Thus any analytical model illustrating the physics of these features is always useful. Therefore we hope that the analyses of nonlinear waves conducted in the present work may provide some insight for understanding these features.

This work extends a previous analysis [2] and examines the dynamics in more general settings where the background matter is not static. We find that in a very special situation where the background matter is expanding at a particular rate and has a density less than the critical value the gravitational sound waves exist in the form of solitary wave trains. Furthermore, we also find that an expansion slightly deviating from this special rate can make the gravitational sound waves change drastically, where the waves immediately undergo transitions to become highly nonlinear in the form of isolated solitons. Sizable density oscillations are also found in most solitons, which may be identified as the multiple mass shells.

(In this paper, the terms solitons and solitary wave trains are used in a rather loose sense. By ''solitons'' we refer to localized nonlinear density enhancement. This definition is certainly not what mathematicians may agree on since we have not shown whether the present soliton solutions may obey the conservation laws upon collisions of solitons.)

This paper is organized as follows. Section II contains the mathematical formulation of the self-similar time-dependent solutions. In Sec. III, the water-bag model [16] used in a previous work for representing a collisionless system is extended to comply with the self-similar scaling [2]. The analytical result for the wave solution is obtained in Sec. IV and the results for the solitons are presented in Sec. V. Finally, we give conclusions in Sec. VI, which discusses the astrophysical implications of these solutions. The Appendix briefly reviews the nonlinear waves in a static background.

II. MATHEMATICAL FORMULATION FOR SELF-SIMILAR STRUCTURES IN EXPANDING AND CONTRACTING FLUIDS

We consider a physical situation where the collisionless fluid expands or contracts uniformly in two directions, say,

the x and y directions, and the nonlinear waves propagate in the z direction. First, we may decompose the gravitational potential ϕ into two components

$$\phi(\mathbf{x},t)=\psi(z,t)+\frac{1}{2}[D_x(t)x^2+D_y(t)y^2], \qquad (1)$$

where ψ accounts for the amount of gravity in the z direction and the second term for that in the other two directions. The quantities $D_x(t)=d_x/t^2$ and $D_y(t)=d_y/t^2$ can be related to the expanding or contracting rates in the x and y directions and are inversely proportional to t^2 with the proportional constants d_x and d_y. To understand Eq. (1) we may examine the Poisson equation

$$\nabla^2\phi=4\pi G\rho \qquad (2)$$

and thus

$$\frac{d^2\psi}{dz^2}=4\pi G\rho-(D_x+D_y). \qquad (3)$$

The time dependence (t^{-2}) of D_x and D_y can be obtained by considering the dynamics transverse to the z direction. For a collection of collisionless particles, we may write their momentum equation as

$$\rho\left(\frac{\partial V_i}{\partial t}+V_j\frac{\partial V_i}{\partial x_j}\right)=-\frac{\partial P_{ij}}{\partial x_j}-\rho\frac{\partial\phi}{\partial x_i} \qquad (4)$$

in tensor notation, where the repeated indices sum. The quantity P_{ij} is a symmetric stress tensor and chosen also to be a diagonal tensor for this work. The velocity components in the x and y directions can be solved for straightforwardly if the stress tensor has no variation in these two directions and the velocity components in these two directions do *not* depend on z. Let $D_i=d_i/t^b$ and the momentum equation perpendicular to z reads

$$\frac{\partial V_i}{\partial t}+V_j\frac{\partial V_i}{\partial x_j}=-\frac{x_id_i}{t^b},$$

where the repeated indices on the right-hand side do not sum and i runs only over 1 and 2. To obtain a general solution containing a power-law time dependence requires that $b=2$ and the solution be expressed as

$$V_x=\frac{h_xx}{t}, \qquad V_y=\frac{h_yy}{t}, \qquad (5)$$

in which the constants h_x and h_y are related to d_x and d_y through the equalities

$$d_x=h_x-h_x^2, \qquad d_y=h_y-h_y^2. \qquad (6)$$

The first requirement thus fixes the t^{-2} dependence for $\mathbf{D}$.

Because of the power-law time dependence of $\mathbf{D}$, Eq. (3) hints at the possible existence of nonlinear solutions that are separable in the independent variables t and z, for which the time dependence of all variables is in the form of a power law. Proceeding in this direction, first we must employ a change of independent variables from (t,z) to a set of self-similar variables (τ,η),

$$t=\tau, \qquad z=\eta\tau^\alpha, \qquad (7)$$

where α is a free parameter. It follows that

$$\frac{\partial}{\partial z}=\tau^{-\alpha}\frac{\partial}{\partial\eta}, \qquad \frac{\partial}{\partial t}=\frac{\partial}{\partial\tau}-\frac{\alpha\eta}{\tau}\frac{\partial}{\partial\eta}. \qquad (8)$$

In addition, we must assume that ρ, V_z, and ψ all have the power-law time dependence

$$\rho=n(\eta)\tau^{-2}, \qquad V_z=u_z(\eta)\tau^\beta,$$

$$\psi=\chi(\eta)\tau^{-2+2\alpha}, \qquad P_{33}=p(\eta)\tau^\gamma, \qquad (9)$$

where β and γ are pure numbers and P_{33} is the (z,z) component of the pressure tensor in a collisionless system. The τ^{-2} dependence of ρ is required by Eq. (3) to be consistent with the same time dependence of $\mathbf{D}$. In addition, the time dependence of ψ is also obvious, as required by Eq. (3).

Under these assumptions, the momentum equation in the z direction can be cast into the form

$$\tau^{\beta-1}\left(\beta u_z-\alpha\eta\frac{du_z}{d\eta}\right)+\tau^{2\beta-\alpha}u_z\frac{du_z}{d\eta}$$

$$=-\tau^{\gamma-\alpha+2}n^{-1}\frac{dp}{d\eta}-\tau^{-2+\alpha}\frac{d\chi}{d\eta} \qquad (10)$$

and the continuity equation

$$\frac{\partial\rho}{\partial t}+\frac{\partial}{\partial x_i}(\rho V_i)=0 \qquad (11)$$

becomes

$$\tau^{-3}\left(-2n-\alpha\eta\frac{dn}{d\eta}\right)+\tau^{\beta-\alpha-2}\frac{d(nu_z)}{d\eta}+\tau^{-3}(h_x+h_y)n=0, \qquad (11')$$

where the last term in Eq. (11') accounts for $\nabla_\perp\cdot(n\mathbf{V}_\perp)$ of Eq. (11). If we demand that all terms in Eqs. (10) and (11') separately have the same time dependence, it follows that

$$\beta-1=2\beta-\alpha=\gamma-\alpha+2=\alpha-2 \qquad (12)$$

and

$$-3=\beta-\alpha-2, \qquad (12')$$

which yield

$$\beta=\alpha-1, \qquad \gamma=2\alpha-4. \qquad (13)$$

These power indices can be completely determined as long as we fix an appropriate equation of state.

III. EQUATION OF STATE FOR COLLISIONLESS PARTICLES

Determination of the equation of state that relates the pressure P_{33} to the mass density ρ for a collisionless system is widely known as not being a straightforward matter. Nevertheless, for an one-dimensional system, a so-called
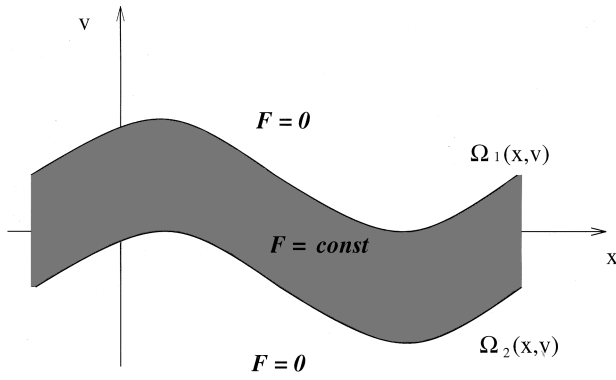
FIG. 1. Phase-space diagram of a typical water-bag model for the distribution function of a collisionless system. The phase-space density is uniform and nonzero within the boundaries Ω_1 and Ω_2 (the shaded region). The rest of the area has zero phase-space density.

water-bag model has been proposed in the past and successfully applied to describing collisionless plasmas [17,18]. Recently, this model has been investigated also in the context of collisionless gravitational sound waves [2]. We will briefly review the formulations in constructing the appropriate equation of state within the context of the water-bag model. In addition, we will extend the formulation to situations where the water bag evolves self-similarly in accordance with the above scaling relations.

The key physics of the collisionless system are that the phase-space distribution function $F(\mathbf{v},\mathbf{x},t)$ is frozen in the phase-space fluid elements and the phase-space elements evolve as if they were incompressible fluids. The water-bag model is designed to capture these essential features in a simple and relatively tractable manner.

The water-bag model considers a special initial configuration for the distribution function $F(\mathbf{v},\mathbf{x},t)$, which assumes only two values in the phase space: either 0 or a constant F_0. Since the boundary separating 0 and F_0 is frozen in the phase-space fluids, the boundary acts as if it were a deformable bag that separates the incompressible, constant-density water within the bag from a vaccum outside. The subsequent evolution of the distribution function is reduced to nothing more than that of each boundary with the index n. (See Fig. 1 for an example of a two-boundary water bag.) The boundary n assumes the form $\mathbf{v}=\Omega_n(\mathbf{x}(t))$ as long as Ω_n remains a single-valued function. We may project the phase-space distribution function $F(\mathbf{v},\mathbf{x},t)$ to the $(v_z,\mathbf{x})$ space to obtain a reduced distribution function $f_z(v_z,\mathbf{x},t)$ $[\equiv \int F(\mathbf{v},\mathbf{x},t)d\mathbf{v}_\perp]$. As long as the wave dynamics is in only the z direction and the background expands or contracts uniformly according to Eq. (5), the reduced one-dimensional distribution function is independent of $\mathbf{x}_\perp$ and can be trivially related to original distribution function through

$$F(\mathbf{v},\mathbf{x},t)=f_z(v_z,z,t)f_\perp(\mathbf{v}_\perp,\mathbf{x}_\perp,t),\qquad(14)$$

with

$$f_\perp(\mathbf{v}_\perp,t)=\left[\Theta\left(a_xv_x-\dot{a}_xx+\frac{c_x}{2}\right)-\Theta\left(a_xv_x-\dot{a}_xx-\frac{c_x}{2}\right)\right]$$
$$\times\left[\Theta\left(a_yv_y-\dot{a}_yy+\frac{c_y}{2}\right)-\Theta\left(a_yv_y-\dot{a}_yy-\frac{c_y}{2}\right)\right],$$
$$(15)$$

where Θ is the Heaviside step function, $a_x(t)$ and $a_y(t)$ are time-dependent scaling factors in the x and y directions, respectively, and c_x and c_y are constants, the thermal widths at some reference time.

It can be shown straightforwardly that this distribution function satisfies the collisionless Boltzmann equation

$$\left[\frac{\partial}{\partial t}+\mathbf{v}_\perp\cdot\frac{\partial}{\partial\mathbf{x}_\perp}-\frac{d_xx}{t^2}\frac{\partial}{\partial v_x}-\frac{d_yy}{t^2}\frac{\partial}{\partial v_y}\right]f_\perp=0\qquad(16)$$

by direct substitution provided that

$$\ddot{a}_x=-\frac{d_x}{t^2}a_x,\qquad\ddot{a}_y=-\frac{d_y}{t^2}a_y.\qquad(17)$$

Note that Eq. (17) yields the solutions

$$a_x=t^{h_x},\qquad a_y=t^{h_y},\qquad(18)$$

where h_x and h_y are given by Eq. (6). Thus the above formulation can self-consistently describe the uniform expansion of collisionless particles in the transverse direction. Generalization to a three-dimensional uniform expansion for any arbitrary distribution is a standard exercise in cosmology.

What remains to be worked out is the dynamics in the z direction, and this is where the power of the water-bag model lies. Given Eq. (14) for F, the mass density can be expressed as

$$\rho(z,t)=\int F(\mathbf{v},\mathbf{x},t)d\mathbf{v}_\perp dv_x=\frac{c_xc_y}{a_xa_y}\int f_z(v_z,z,t)dv_z$$
$$=F_0\frac{c_xc_y}{a_xa_y}[\Omega_{z,1}(z,t)-\Omega_{z,2}(z,t)],\qquad(19)$$

the mass flow velocity as

$$\mathbf{V}(z,t)=\frac{\int\mathbf{v}F(\mathbf{v},\mathbf{x},t)d\mathbf{v}_\perp dv_z}{\rho(z,t)}=\hat{z}\frac{\Omega_{z,1}(z,t)+\Omega_{z,2}(z,t)}{2}$$
$$+\hat{x}\frac{x\dot{a}_x}{a_x}+\hat{y}\frac{y\dot{a}_y}{a_y},\qquad(20)$$

and the pressure tensor as

$$P_{ij}(z,t)=\int(v_i-V_i)(v_j-V_j)F(\mathbf{v},\mathbf{x},t)d\mathbf{v}_\perp dv_z.\quad(21)$$

P_{ij} can be shown to be a diagonal tensor. The relevant component to be used later is

$$P_{33}(z,t)=\frac{F_0c_xc_y[\Omega_{z,1}(z,t)-\Omega_{z,2}(z,t)]^3}{24a_x(t)a_y(t)}.\qquad(22)$$

In Eq. (19) we have let the mass of the particle be unity without loss of generality since the gravitational constant G can be properly adjusted to accommodate this choice of mass.

Note that Eq. (5) for the perpendicular flow velocity is recovered with the help of Eq. (18). We also obtain $P_{xx} = c_x^2 \rho / 24 a_x^2$ and $P_{yy} = a_y^2 \rho / 24 a_y^2$

Equations (19) and (22) are then combined to yield the desired equation of state for the collisionless dynamics in the z direction:

$$P_{33}(z,t) = \frac{\rho^3(z,t) a_x^2(t) a_y^2(t)}{24 F_0^2 c_x^2 c_y^2} = \kappa \rho^3(z,t) t^{2(h_x + h_y)}, \quad (23)$$

where κ is a constant and can be regarded as an effective entropy. Armed with Eq. (23), we may return to Eq. (9) and find that

$$\gamma = 2(h_x + h_y - 3) \quad (24)$$

and therefore the parameters α and β are completely fixed with the help of Eq. (13):

$$\alpha = h_x + h_y - 1, \quad \beta = h_x + h_y - 2. \quad (25)$$

The constant rates of perpendicular expansion h_x and h_y turn out to be the only two free parameters in our problem.

IV. SOLITARY WAVE TRAINS

The final step of our manipulations entails integration of both Eqs. (3) and (11) with respect to η once. It yields

$$\frac{d\chi}{d\eta} = \frac{4\pi G}{3 - 2(h_x + h_y)}[u_z - (h_x + h_y - 1)\eta]n - (d_x + d_y)\eta. \quad (26)$$

Substituting Eqs. (6) and (26) into Eq. (10), we may obtain a set of two first-order ordinary differential equations for $u_z(\eta)$ and $n(\eta)$. In fact, a more illuminating set of equations can be obtained by replacing the variable u_z in favor of the mass flux in an expanding frame of reference $n[u_z - (h_x + h_y - 1)\eta]$, where $(h_x + h_y - 1)\eta$ is the expanding pattern speed of the waves. The governing equations then become

$$\frac{dq}{d\xi} = \frac{q^3}{s^2 - 3q^4}\left(\frac{2s}{3[3 - 2(h_x + h_y)]} \right.$$

$$\left. - [h_x + h_y - h_x^2 - h_y^2 - (h_x + h_y - 1)(h_x + h_y - 2)]\xi \right)$$

$$(27)$$

and

$$\frac{ds}{d\xi} = [3 - 2(h_x + h_y)]q, \quad (28)$$

where $q \equiv n/n_c$, $\xi \equiv \eta/n_c\sqrt{\kappa}$, $s \equiv n[u_z - (h_x + h_y - 1)\eta]/n_c^2\sqrt{\kappa}$, and $n_c \equiv 1/6\pi G$. The matter density is normalized to the critical density and the length to the Jeans length associated with the critical density.

This set of nonlinear equation is generally nonintegrable. However, we may locate two special parameter regimes for which the equations are integrable. These correspond to particular choices for the parameters h_x and h_y.

First, we may let the coefficient of ξ on the right-hand side of Eq. (27) be zero and Eqs. (27) and (28) become autonomous. The procedure for seeking solutions is standard. Divide Eq. (27) by Eq. (28) to form a first-order differential equation, where s^2 can be regarded as the dependent variable and $1/q$ as an independent variable, and one finds that it becomes a linear equation, for which s can be expressed as an analytical function of q in terms of the exponential integral. Unfortunately, q is a double-valued function of s and the solution always runs into the point where $dq/ds = \infty$. This corresponds to the sonic singularity at $s^2 = 3q^4$ at which the right-hand side of Eq. (27) diverges. This class of solution is unphysical and we shall discard it. In this regard, we shall see later that the soliton solutions must also encounter the same singular denominator; however, the numerator on the right-hand side of Eq. (27) can actually be adjusted to make the combined term finite. Therefore, the soliton solution can pass smoothly through the sonic transition, representing a physical solution.

Second, let

$$h_x + h_y = \tfrac{3}{2}. \quad (29)$$

Although Eq. (28) seems to yield $s = $ const, the right-hand side of Eq. (27) diverges. To avoid such a pathological situation, we may demand that $s \to 0$ as $h_x + h_y \to \tfrac{3}{2}$ in order to keep the quantity $s/[3 - 2(h_x + h_y)]$ finite. Defining $S \equiv s/[3 - 2(h_x + h_y)] - k\xi$, where $k \equiv 3(3h_x - 2h_x^2 - \tfrac{1}{2})/2$, we find that Eqs. (28) and (29) become

$$\frac{dq}{d\xi} = -\frac{2S}{9q} \quad (30)$$

and

$$\frac{dS}{d\xi} = q - k. \quad (31)$$

Equations (30) and (31) are combined to yield

$$\frac{d^2S}{d\xi^2} = \frac{-2S}{9(k + dS/d\xi)}, \quad (32)$$

which can be integrated once with a standard technique by multiplying both sides by the factor $1/(dS/d\xi)$ and using the chain rule. It follows that

$$\frac{d}{dS}\left(\frac{dS}{d\xi} \right) = \frac{-2S}{9(k + dS/d\xi)(dS/d\xi)} \quad (33)$$

or

$$\left(\frac{1}{k}\frac{dS}{d\xi} \right)^3 + \frac{3}{2}\left(\frac{1}{k}\frac{dS}{d\xi} \right)^2 + \frac{S^2}{3k^3} = \frac{c_0}{3}, \quad (34)$$

where c_0 is an integration constant. The quantity $dS/d\xi$ can be solved for from the cubic equation (34) as a function of S. Among the three roots, the physical roots are
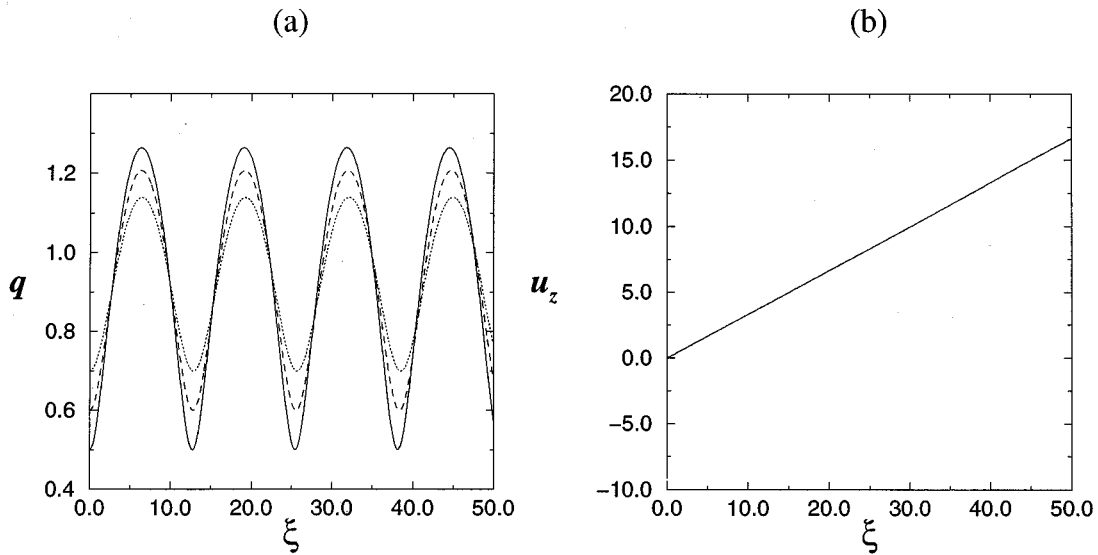
(a)   (b)

FIG. 2. Typical solitary wave trains. (a) Normalized densities q and (b) flow speeds u_z. The solid, dashed, and dotted lines are for $c_0 = 0.67$, 0.44, and 0.24, respectively. The three flow speeds u_z almost coincide in this plot.

$$\frac{1}{k}\frac{dS}{d\xi} = -\left(\frac{Q_1+Q_2}{2}+\frac{a}{3}\right)+\sqrt{\frac{3i}{a}}(Q_2-Q_1) \qquad (35)$$

and

$$\frac{1}{k}\frac{dS}{d\xi} = -\left(\frac{Q_1+Q_2}{2}+\frac{a}{3}\right)-\sqrt{\frac{3i}{a}}(Q_2-Q_1), \qquad (35')$$

where

$$Q_1(S) \equiv \left[\frac{1}{12}\left(\frac{S^2}{k^3}-c_0\right)-\frac{Q_0}{108}-\frac{i}{18}\sqrt{\left(c_0-\frac{S^2}{k^3}\right)Q_0}\right]^{1/3},$$

$$Q_2(S) \equiv \left[\frac{1}{12}\left(\frac{S^2}{k^3}-c_0\right)-\frac{Q_0}{108}+\frac{i}{18}\sqrt{\left(c_0-\frac{S^2}{k^3}\right)Q_0}\right]^{1/3},$$

and

$$Q_0(S) \equiv 9\left(\frac{3}{2}-c_0+\frac{S^2}{k^3}\right) \qquad (36)$$

provided that $c_0-S^2/k^3 \geq 0$ and

$$c_0 \leq \tfrac{3}{2}. \qquad (37)$$

The resulting equation can thus be integrated once again where the integration goes from one root to the other when the two roots merge, which occurs when $S^2/k^3 = c_0$ or $Q_0 = 0$. The solution is an anharmonic oscillation $S(\xi) = S_0 + \Delta S(\xi)$, with S_0 being the mean and ΔS purely oscillatory as shown in Fig. 2. The mean $S_0 = 0$ because the solution oscillates about $S=0$. The oscillation ΔS can be reduced to a linear wave in the small-amplitude limit when $c_0 \to 0$ from above. In this limit one can expand $c_0 - S^2/k^3$ as a small parameter and find that $dS/d\xi$ satisfies the standard form of oscillation

$$\frac{1}{2}\left(\frac{1}{k}\frac{dS}{d\xi}\right)^2 + \frac{S^2}{9k^3} = \frac{c_0}{9}. \qquad (38)$$

In general cases, the oscillation amplitude is $|\Delta S| = \sqrt{k^3 c_0}$ even in the nonlinear regime. The amplitude increases with c_0; however, there is an upper limit that c_0 can reach. The value c_0 is bounded by $\frac{3}{2}$ according to Eq. (37) and the maximum amplitude for the nonlinear oscillations becomes

$$|\Delta S|_{\max} = \sqrt{\frac{3k^3}{2}}. \qquad (39)$$

One may determine the maximum amplitude for $dS/d\xi$ as well. Note from Eq. (31) that the density is

$$q = k + \frac{dS}{d\xi},$$

which must be non-negative. The maximum of $-dS/d\xi$ is therefore k, occurring at $S=0$. Replacing $dS/d\xi$ by $-k$ and S by 0 in Eq. (34), we find that c_0 is also bounded from above, which is incidentally identical to Eq. (37). Thus maximum-amplitude oscillations for the solitary wave yield periodic vacuum states.

The mean background density is

$$\langle q \rangle = k = \frac{3(3h_x - 2h_x^2 - \frac{1}{2})}{2} \leq \frac{15}{16}, \qquad (40)$$

where the equality holds when $h_x = h_y = \frac{3}{4}$, an isotropic perpendicular expansion. Thus the average density $\langle n \rangle$ is always less than the critical density n_c. In the regime that gives physical solutions, we demand that $k>0$ or

$$\frac{3-\sqrt{5}}{4} \leq h_x \leq \frac{3+\sqrt{5}}{4}. \qquad (41)$$

For a very underdense local universe, h_x should approach the two bounds given by Eq. (41) and the perpendicular expansion in x and y exhibits extreme anisotropy. However, for all values of h_x within the bounds of Eq. (41), we always find that
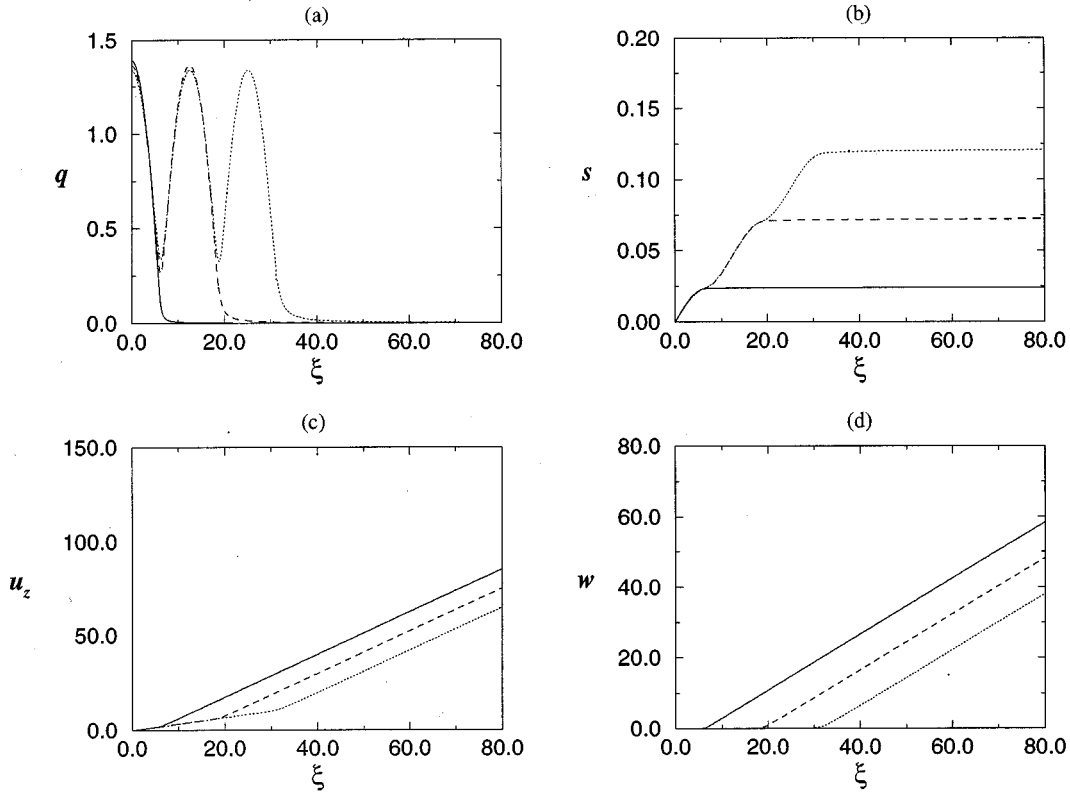
FIG. 3. Solitons of the odd-period solution for $h_\perp = 0.749$. (a) Normalized densities q, (b) normalized mass fluxes s, (c) flow speeds u_z, and (d) flow speeds relative to the pattern speeds w. The solid, dashed, and dotted lines are for $q(0) = 1.393, 1.365$, and 1.34, respectively.

$$u_z = \frac{\eta}{2} . \tag{42}$$

The inequality (41) will be referred to again in the discussion of the soliton solutions in the next section since the most interesting soliton solutions mimicking the multiple mass shells are near this range of expansion rates. Interestingly, we also notice that when $h_x = \frac{1}{2}$ and $h_y = 1$, the background can expand isotropically in the x and z directions, but not in the y direction, with a mean density $\langle n \rangle = 3 n_c / 4$.

V. SOLITON SOLUTIONS ($h_\perp \equiv h_x = h_y$)

For the sake of demonstrating the key physics of the solitons, we shall now focus on the case of isotropic perpendicular expansion where $h_x = h_y = h_\perp$. The extension to the general anisotropic cases is straightforward. We first examine what happens when Eq. (29) is slightly violated, for which $\epsilon \equiv h_\perp - \frac{3}{4} \ll 1$. The coupled equations, (27) and (28), are generally nonintegrable; however, as $\epsilon \to 0$, we expect that the solutions to Eqs. (27) and (28) should in some way resemble the integrable solitary wave solution obtained earlier. One notes that the solitary wave solution ($\epsilon = 0$) contains a subsonic flow, where the denominator of Eq. (27) is always a negative definite quantity. In the present case, where ϵ is not zero, it is possible that the denominator can turn from a negative value to a positive value at some large ξ if the quantity s grows with the distance ξ. In this case, the solutions, originally not much different from the solitary waves, can undergo a drastic qualitative change as the denominator crosses zero. This rapid transition will give rise to a qualita-

tively very different solution from the solitary wave.

With this qualitative understanding in mind, we carry out the numerical integration for Eqs. (27) and (28). A second-order Runge-Kutta integration scheme has been adopted. This set of nonlinear differential equations possesses parity symmetry, in that q can be symmetric and s antisymmetric upon the reflection of ξ. This symmetry property fixes a boundary condition $s(\xi = 0) = 0$. Another boundary condition is given by the requirement that the solution be nonsingular at the trans-sonic point where the denominator of Eq. (27) vanishes. A shooting technique is used for the integration, starting from the boundary $\xi = 0$. This is a nonlinear eigenvalue problem with $q(0)$ being the eigenvalue.

It turns out that there are two types of soliton solution for each value of $h_\perp$, where the number of oscillations prior to the rapid transition at the sonic point can be either odd or even integers. (Note that since the soliton has reflectional symmetry the oscillations on the both sides of $\xi = 0$ must be included in the counting.) Plotted in Figs. 3 and 4 are the typical solutions for the two types of soliton solutions at the expansion rate $h_\perp = 0.749$ or $\epsilon = -10^{-3}$. Both figures contain three different eigensolutions, which correspond to different nonlinear eigenvalues $q(0)$. (We have not exhausted all eigenfunctions for this choice of $h_\perp$.) Not far from the boundary $\xi = 0$, the solution closely resembles the solitary waves of Sec. IV. However, at a large ξ, the solution abruptly makes a transition to a low-density, high-speed state.

For this particular choice of $h_\perp$, each type of solution contains only three eigenfunctions corresponding to either period-1, period-3, and period-5 solutions or period-2,
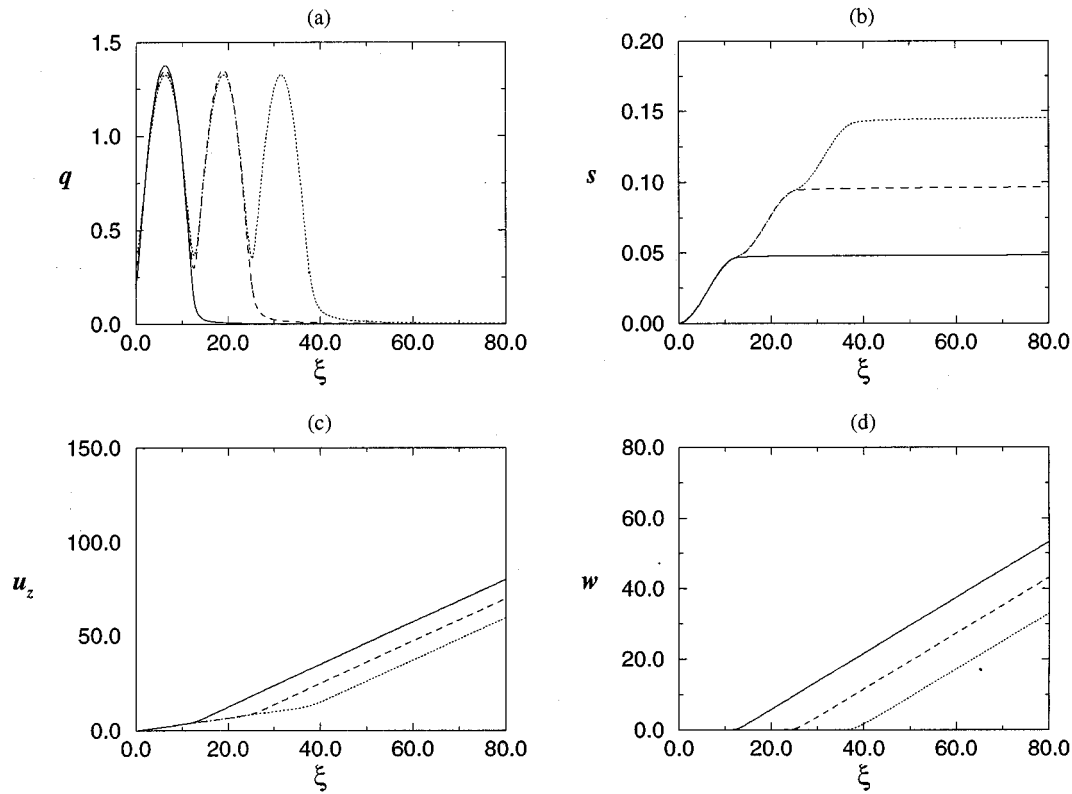
FIG. 4. Solitons of the even-period solution for $h_\perp = 0.749$. The panels are the same as in Fig. 3. The solid, dashed, and dotted lines are for $q(0) = 0.22$, 0.307, and 0.371, respectively.

period-4, and period-6 solutions. Such solutions represent expanding material slabs embedded in a low-density background and these material slabs can be regarded as one-dimensional solitons. The expansion of the slab pattern is driven by the upstream matter pressure. Figures 3(d) and 4(d) shows that the relative flow speed w is positive throughout the entire region. This means that the velocity u_z is always greater than the soliton pattern speed $\tau^{-\beta}(\partial z/\partial \tau) = (2h_\perp - 1)\eta$, according to Eqs. (7), (9), and (25), indicating that the disks are losing masses to the background.

Plotted in Figs. 5 and 6 are the cases for $\epsilon = 10^{-3}$, where s becomes negative throughout the entire region. Despite the fact that the flow speed relative to the pattern speed w is always negative, the flow speed in the laboratory frame u_z can be both positive and negative. This illustrates that the matter in the disks tend to expand, driving the pattern expansion, but this matter, at some finite distance, must collide with the materials falling in from the background. These solutions represent another situation where the solitons grow to become more massive by collecting the background matter. All soliton solutions show smooth behaviors at the sonic transition, resulting from the fact that both the denominator and numerator in Eq. (27) pass through zero simultaneously. This reflects that the relative flow velocity s/q, starting from the subsonic (supersonic) region, smoothly accelerates (decelerates) to supersonic (subsonic) speeds by the particle pressure in the high-density slab. The slab thus loses (gains) mass to (from) the background.

Our numerical integration finds both period-1 and period-2 soliton solutions down to $\epsilon = -\frac{1}{12}$, where $h_\perp = \frac{2}{3}$, the

Hubble expansion, and the period-1 solution up to $\epsilon = 0.06$, but the period-2 solution up to $\epsilon = 0.04$. As $|\epsilon|$ increases from zero, the number of eigenfunctions decreases, with the sequential disappearance of the many-period solutions down to the period-2 and finally period-1 solutions. At a certain point the period-1 solution is lost completely. The precise range of ϵ, beyond which soliton solutions no longer exist, is relatively difficult to locate since Eqs. (27) and (28) are nonlinear singular equations and the solution can become highly chaotic. Consequently, a higher-order integration scheme does not help improve the accuracy of the solutions near the sonic points. The range of ϵ given above is a conservative estimate.

Plotted in Figs. 7 and 8 are the period-1 solutions and period-2 solutions, respectively, for three different values of $h_\perp$. These figures show some tendencies of the solitons. First, the sonic point moves inwards as ϵ increases. When $h_\perp \rightarrow \frac{2}{3}$, only the period-1 and period-2 solutions survive and the top of the soliton has an almost flat-top density up to very large distances before it drops to match the asymptotic solution described below. This implies the existence of a disk of large thickness, within which the matter expands almost according to the Hubble law and its density is nearly critical. Second, we may also refer to Fig. 9 to assist in detecting another tendency. Plotted in Fig. 9 are the nonlinear eigenvalues $q(0)$ of the period-1 and period-2 solutions versus the perpendicular expansion rates $h_\perp$. The soliton density of the period-1 (period-2) solutions at the core $q(0)$ first increases (decreases) toward decreasing ϵ, and after ϵ becomes negative, the tendency reverses and the top density $q(0)$ decreases (increases).
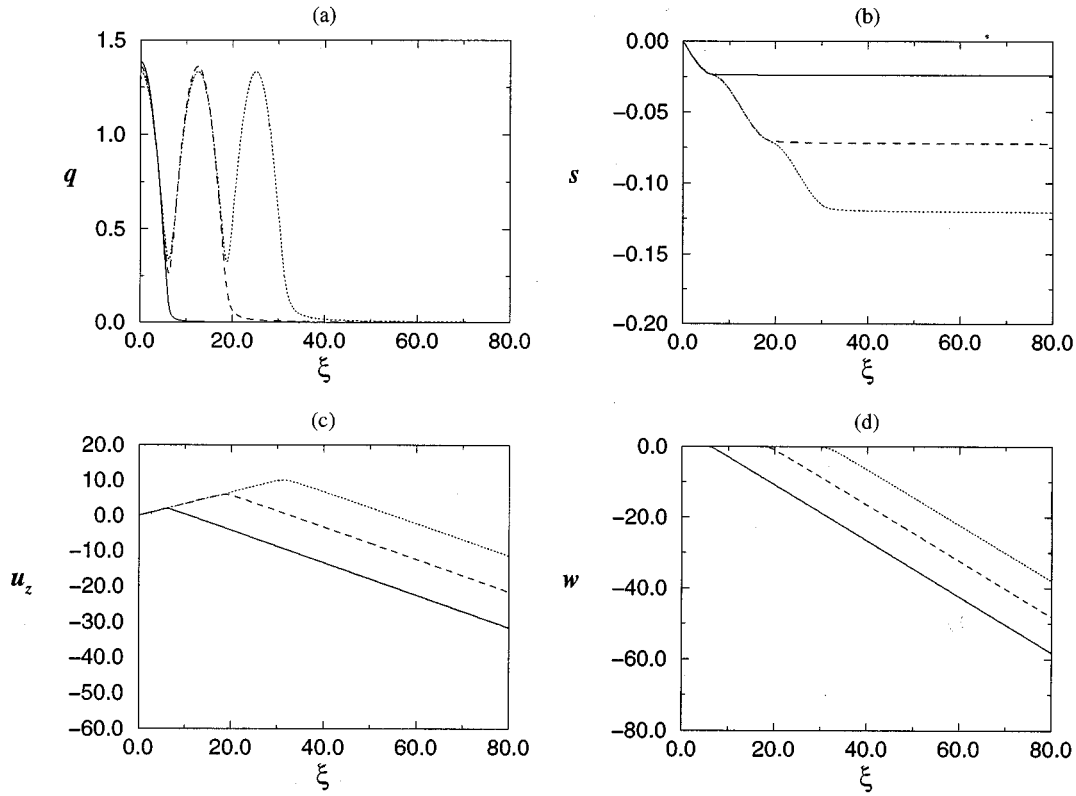
FIG. 5. Solitons of the odd-period solution for $h_\perp = 0.751$. The panels are the same as in Fig. 3. The solid, dashed, and dotted lines are for $q(0) = 1.338, 1.36$, and 1.335, respectively.

The asymptotic supersonic regime of the soliton solutions can be roughly analyzed as follow. In Eq. (27) we ignore the pressure term $3q^4$ in the denominator and the gravity term, proportional to s, in the numerator. Equation (27) then becomes

$$\frac{dq}{d\xi} = \frac{2q^3\xi[h_\perp - h_\perp^2 - 2(h_\perp - 1/2)(h_\perp - 1)]}{s^2}. \quad (43)$$

By inspection, we find that Eq. (43) is homogeneous in that it allows for a power-law solution where

$$s = s_0\xi^\lambda, \quad q = \frac{s_0\lambda}{3 - 4h_\perp}\xi^{\lambda - 1}. \quad (44)$$

Substituting the power-law solution into Eq. (43), we obtain

$$\lambda = \frac{-1 \pm \sqrt{1 + 4a}}{2a}, \quad (44')$$

where $a \equiv 2(3h_\perp - 1)(1 - h_\perp)/(3 - 4h_\perp)^2$. The flow velocity in the comoving frame follows

$$w = \frac{s}{q} = \frac{3 - 4h_\perp}{\lambda}\xi, \quad (45)$$

a linear expansion. Note that such an asymptotic flow has a kinetic energy density

$$\frac{qu_z^2}{2} = \frac{s_0\xi^2}{2(3 - 4h_\perp)}\left(\frac{3 - 4h_\perp}{\lambda} + \frac{1}{3}\right)^2, \quad (46)$$

which is of the order of the asymptotic potential-energy density, proportional to $\int(\int \rho\, dx)dx \propto \int s\, d\xi \propto \xi^{\lambda + 1}$. The value of λ can be shown to be less than unity and therefore the asymptotic total-energy density (propotional to $\xi^{1+\lambda}$) is always smaller than that of the homogeneous and isotropic expansion (propotional to ξ^2) at large distances.

VI. DISCUSSION AND CONCLUSIONS

This work addresses the nonlinear wave characteristics in an expanding local universe filled with collisionless dark matter. Two classes of waves are found: solitary wave trains and solitons. The length scales of both waves are typically of order the Jeans length associated with the critical density. The density ratio $\delta\rho/\langle\rho\rangle$ of the solitary waves remains constant in time, indicative of stable waves, as expected from the notion that their length scale is about the Jeans length. Although similar conclusions can be drawn also for the solitons, the matter within the solitons can be either continuously lost to, or collected from, a much-lower-density background. The solitons therefore can become either less or more massive as time progresses.

A. Solitons

As far as the astrophysical implications of these waves are concerned, the soliton solutions may describe a certain phase of nonlinear evolution for high-density sheets in the collapsing disk scenario of large-scale structure formation [6–11]. At the deep nonlinear stage of the disk collapse, sheetlike density caustics can form [6,19]. While matter is compressed
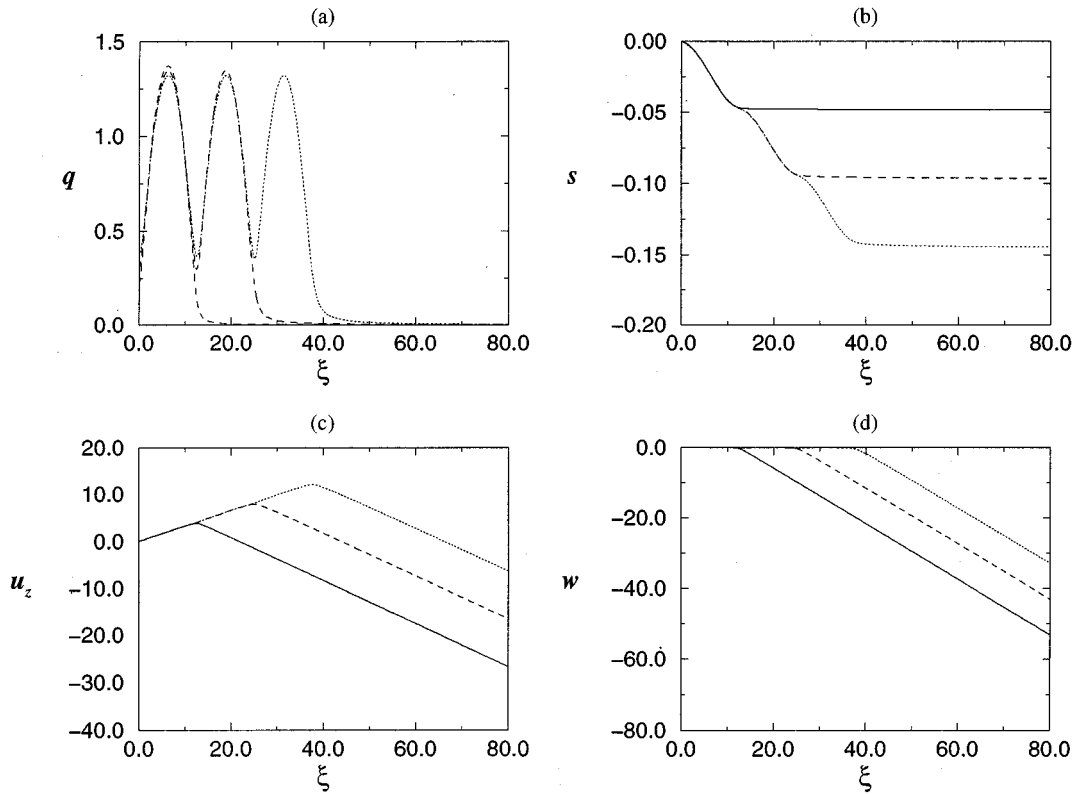
FIG. 6. Solitons of the even-period solution for $h_\perp = 0.751$. The panels are the same as in Fig. 3. The solid, dashed, and dotted lines are for $q(0) = 0.22, 0.307$, and 0.372, respectively.

in one direction, it may expand in the other two directions. This configuration sets up an initial condition for the post-collapse rebound phase to begin. The hot and dense slab expands outward, where either the disk matter can be pressured out of the hot slab at supersonic speeds and blend with the much-lower-density background Hubble flow or the background matter falls back into the expanding slab, leading to an increasingly massive disk. Interestingly, we note that near the perpendicular expansion rate $h_\perp \sim \frac{3}{4}$ the expanding disk exhibits periodic density depressions at sizable levels, as illustrated in Fig. 8 for an extreme doubled-sheet case, where $h_\perp = 0.7501$. Many-period soliton solutions can actually exist for this value of $h_\perp$. In fact, if we are not limited to the isotropic perpendicular expansion, there is a finite range of h_x and h_y, which are related by $h_x + h_y \approx \frac{3}{2}$, that yields the many-period soliton solutions. The range is approximately identical to that for the solitary waves indicated in Eq. (41).

This type of multiple-mass-shell solution has been believed to be the basis for dissipationless gravitational turbulence arising from multiple-mass-shell crossings [13–15]. The physics beyond such configurations may be traced to instabilities such as the two-stream instability or the inverse Landau damping. As two collisionless mass flows penetrate each other, the free energy associated with the relative motion can be released and vigorously generates fluctuations of length scale the Jeans length. Our multiple mass-shell-solution may represent the nonlinearly saturated states of such instabilities.

To elaborate further the connection of the soliton solution with the post-disk-collapse phase, we notice that the self-similar time scaling assumed in Sec. II begins at the rebound phase, for which we denote its time as t_r. The critical density defined in the previous sections should have referred to this definition of time and been $\rho_c \equiv 1/6\pi G t_r^2$ which is much greater than the cosmological critical density $1/6\pi G t_h^2$ when $t_r \ll t_h$, where t_h is the cosmological age. Although the asymptotic states of these soliton solutions do not contain the background Hubble flow, it is understood that the soliton flows should ultimately match the Hubble flow at some large distances where additional physics, such as shock transitions, is required. Also note that the soliton solutions in this context will become invalid when $t_r \sim t_h$, where $\rho_c \sim 1/6\pi G t_h^2$. Unless the average density of the universe is less than the critical density by a huge factor, it is expected that the description of the disk evolution by the soliton solutions should hold only for a finite range of time.

B. Solitary wave trains

For the implications of the solitary wave trains that exist only in an underdense and anisotropically expanding background, we feel that these solutions are probably of little relevance to the real world unless one is bold enough to challenge the validity of an isotropic universe. This is because the solitary wave trains do not drastically modify the background density and therefore should not be expected to drastically change the background expansion from an isotropic to an anisotropic one. But how can an underdense and
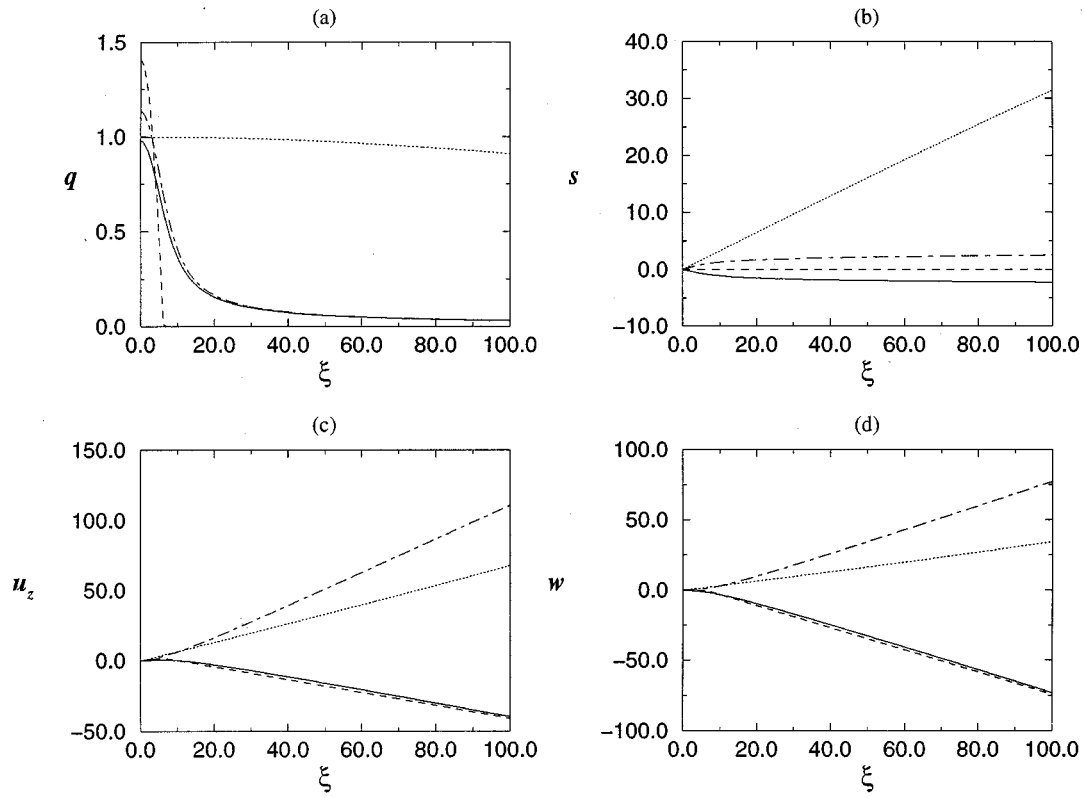
FIG. 7. Period-1 soliton solutions for various values of $h_\perp$. The solid lines are for $h_\perp = 0.79$, the dashed lines for $h_\perp = 0.7501$, the dash-dotted lines for $h_\perp = 0.71$, and the dotted lines for $h_\perp = 0.669$.
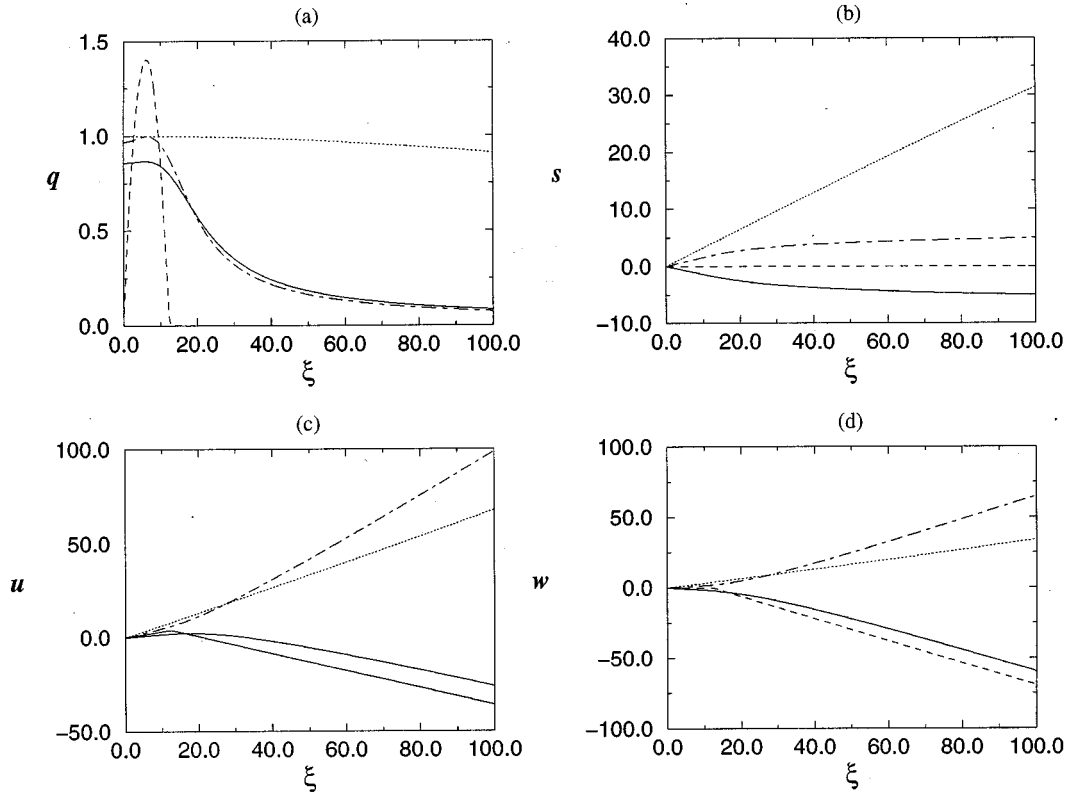

FIG. 8. Period-2 soliton solutions for various values of $h_\perp$. The respective lines are the same as those described in Fig. 7.
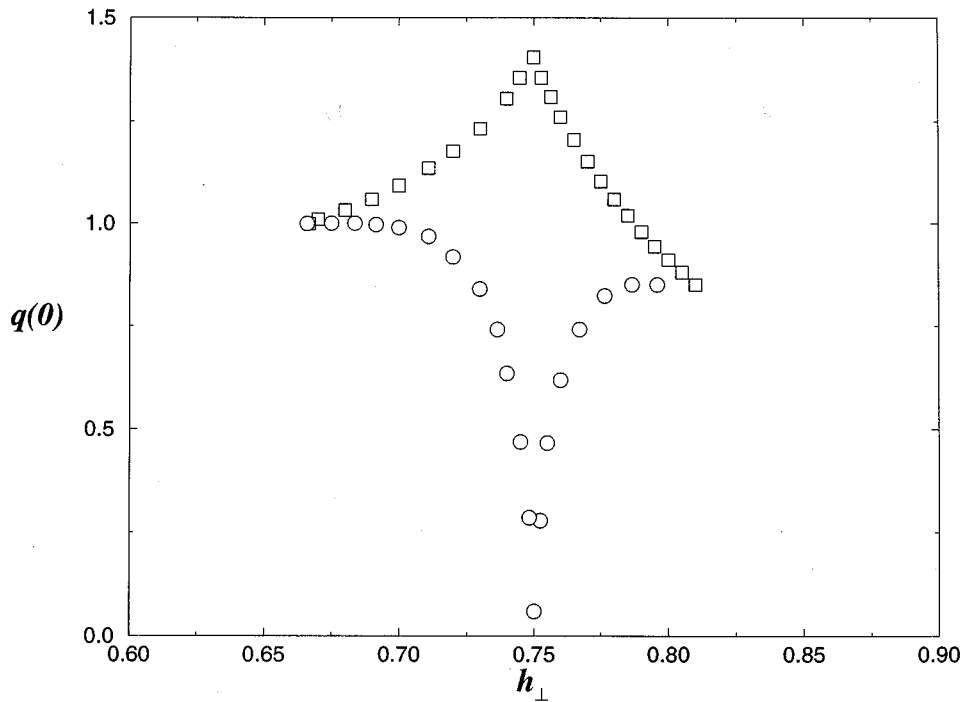
FIG. 9. Parameter space of the nonlinear eigenvalues $q(0)$ for the period-1 (squares) and period-2 (circles) solutions versus the perpendicular expansion rates $h_\perp$.

isotropically expanding local universe, in which we believe we live, support wave fluctuations?

An underdense, homogeneous, and isotropically expanding universe is known to have two stages of evolution [20]: an initial stage where the expansion factor $a(t)$ scales as $t^{2/3}$ (the matter dominated regime) and a late stage where $a(t) \sim t$ (the curvature dominated regime). This time dependence does not satisfy the self-similar time scaling assumed throughout the above analyses, thus explaining why we cannot obtain a solution describing an underdense, homogeneous, and isotropically expanding background configuration. The evolution of waves in such a background can be solved as an initial-value problem. The equation of state described in the first equality of Eq. (23) can be adopted in an approach treating the collisionless particles as a fluid. As for the nonlinear waves, there is probably no straightforward analytical treatment; numerical simulations are probably the only tool for understanding the nonlinear evolution of waves in such a background.

Related to the question of how an underdense universe may evolve, the soliton solutions near $h_\perp = \frac{2}{3}$ may reveal another interesting possibility, in contrast to the conventional answer described in the preceding paragraph. Figures 7 and 8 show the flat-density-top soliton solutions near $h_\perp = \frac{2}{3}$. Although the density will eventually drop to zero at some large distance, within the flat-top region, the density always assumes nearly the critical value and the flow expands almost isotropically at a rate nearly the critical rate. That is, the solution locally looks little different from the Newtonian Hubble flow. This type of solution suggests that if the universe does not have sufficient mass to halt its expansion globally, it may manage to halt the expansion locally. This can be nearly achieved by aggregating most of the mass into a very thick slab, within which the density is sufficiently high and its gravity can just balance the expansion. Such a slab, however, is continuously losing its mass to the nearly empty space outside ($\rho \propto x^{-2/3}$), at a mass flux (propotional to $x^{1/3}$) much less than that of the Hubble flow (propotional to x). As far as the real universe is concerned, in view of the isotropy of the quasar distribution, one may want to look for such interesting solutions for the Einstein equation in spherically symmetric configurations. If such spherically symmetric solutions can indeed be found, they may provide a new challenge for cosmology, in that the universe expansion will be distance dependent and determination of the cosmic time that relies so much on the extrapolation from the current Hubble expansion rate H_0 will be misleading. Indeed, if our galaxy is located well within a large flat-top region of the local universe, it is not easy for the current observations to distinguish such an inhomogeneous universe from the classical homogeneous one.

APPENDIX A: SINGULAR SOLITARY WAVE TRAINS IN A STATIC BACKGROUND [2]

Propagating wave solutions in a static background can be best studied in the wave rest frame of reference. In this reference frame, the system is stationary, although the flow is nonzero. One may treat this problem as a time-independent problem, for which the mass flux, momentum flux, and energy flux are all uniform in order to ensure stationarity. For one-dimensional (z-direction) propagation, these conserved fluxes are

$$\rho V_z = c_0, \qquad (A1)$$

$$T^{03} \equiv \left(\frac{V_z^2}{2} + E(\rho) + \phi \right) \rho V_z = c_1 c_0, \qquad (A2)$$

and

$$T^{33} \equiv \rho V_z^2 + P_{33} + \frac{1}{8\pi G} \left(\frac{d\phi}{dz} \right)^2 = c_2, \qquad (A3)$$

respectively, where c_0, c_1, and c_2 are constants and $E(\rho) \equiv \int dP_{33}/\rho$ is the internal energy. The correspondence to Eq. (23) for the equation of state of collisionless particles reads

$$P_{33} = \kappa \rho^3, \qquad (A4)$$

which can be obtained from Eq. (23) by setting the expansion factors $a_x = a_y = 1$.

Having expressed P_{33} and E as functions of ρ, we are now in a position to solve for $d\phi/dz$ as a function of ϕ algebraically. This can be carried out because we have four unknowns ($d\phi/dz$, ϕ, ρ, and V_z) and three equations [Eqs. (A1), (A2), and (A3)]. Alternatively, one may also solve for $d\rho/dz$ as a function of ρ after some algebraic manipulations. This alternative yields a familiar form

$$\frac{1}{2} \left(l_j \frac{d\rho}{dz} \right)^2 + U(\rho) = 0, \qquad (A5)$$

where

$$U(\rho) \equiv \frac{\rho^5 [\rho^4 - \rho(c_2/\kappa) + (c_0^2/\kappa)]}{[(c_0^2/\kappa) - 3\rho^4]^2}, \qquad (A6)$$

with $l_j \equiv \sqrt{\kappa/8\pi G}$, of order the Jeans length. The solutions to Eq. (A6) are anharmonic oscillations, where ρ is bouncing in between two zeros of $U(\rho)$.

However, we note that this ''potential'' $U(\rho)$ has a second-order pole at the sonic point. It can be shown rigorously that the sonic point must always be located in between the two zeros of $U(\rho)$, meaning that when ρ is bouncing in between the ''potential well'' $U(\rho)$, it always encounters the sonic singularity. The solution may be obtained by considering an analogy to the particle dynamics where a particle may roll down the potential well from one side of the singularity to the other.

Although it may seem that this singularity is rather weak, in that ρ, V_z, and ϕ are all continuous across the sonic point and $d\rho/dz$ and dV_z/dz diverge at the sonic point as $|z - z_s|^{-1/2}$, in fact, a careful analysis shows that $d\phi/dz$ is discontinuous and there must be a negative density spike located at the singularity. It is this negative density spike that makes this solution unphysical, as pointed out by Adams, Fatuzzo, and Watkins in a similar problem for the molecular clouds [21].

[1] V. Trimble, Contemp. Phys. **29**, 373 (1988).

[2] T. Chiueh and T. B. Woo, Chin. J. Phys. **34**, 91 (1996).

[3] T. Padmanabhan, *Structure Formation in the Universe* (Cambridge University Press, Cambridge, 1993).

[4] N. A. Bahcall, L. M. Lubin, and V. Dorman, Astrophys. J. Lett. **447**, L1 (1995).

[5] L. A. Kofman, N. Y. Gnedin, and N. A. Bahcall, Astrophys. J. **413**, 1 (1993).

[6] S. F. Shandarin and Ya. B. Zeldovich, Rev. Mod. Phys. **61**, 185 (1989).

[7] Ya. B. Zeldovich, Astron. Astrophys. **5**, 84 (1970).

[8] A. Sunyaev and Ya. B. Zeldovich, Astron. Astrophys. **20**, 189 (1972).

[9] T. Chiueh, Chin. J. Phys. **32**, 319 (1994).

[10] V. De Lapparent, M. J. Geller, and J. P. Huchra, Astrophys. J. Lett. **302**, L1 (1986).

[11] M. J. Geller and J. P. Huchra, Science **246**, 897 (1989).

[12] A. L. Melott, Astrophys. J. Lett. **426**, L11 (1994).

[13] A. V. Gurevich and K. P. Zybin, Zh. Éksp. Teor. Fiz. **90**, 5 (1988) [Sov. Phys. JETP **67**, 1 (1988)].

[14] A. V. Gurevich and K. P. Zybin, Zh. Éksp. Teor. Fiz. **94**, 3 (1988) [Sov. Phys. JETP **67**, 1957 (1988)].

[15] T. Buchert, G. Karakatsanis, R. Klaffl, and P. Schiller (unpublished).

[16] M. R. Feix, J. P. Doremus, and G. Baumann, in *Gravitational N-Body Problems*, edited by M. Lecar (Reidel, Dordrecht, 1972), p. 347.

[17] T. Katsouleas and W. B. Mori, Phys. Rev. Lett. **61**, 90 (1988).

[18] T. Chiueh and T. C. Lai, Phys. Rev. A **44**, 6944 (1991).

[19] V. I. Arnold, S. F. Shandarin, and Ya. B. Zeldovich, Geophys. Astrophys. Fluids Dyn. **20**, 111 (1982).

[20] H. Bondi, *Cosmology* (Cambridge University Press, Cambridge, 1961).

[21] F. C. Adams, M. Fatuzzo, and R. Watkins, Astrophys. J. **426**, 629 (1994).